

## THREE-DIMENSIONAL WAVY HELIOSPHERIC CURRENT SHEET DRIFTS

C. PEI<sup>1</sup>, J. W. BIEBER<sup>1</sup>, R. A. BURGER<sup>2</sup>, AND J. CLEM<sup>1</sup>

<sup>1</sup> Department of Physics and Astronomy and Bartol Research Institute, University of Delaware, Newark, DE 19716, USA; [pei@physics.udel.edu](mailto:pei@physics.udel.edu)

<sup>2</sup> Centre for Space Research, North-West University, Potchefstroom Campus, Private Bag X6001, Potchefstroom 2520, South Africa

Received 2011 July 6; accepted 2011 October 4; published 2011 December 22

### ABSTRACT

We present an analytic method to determine the directions of the three-dimensional (3D) heliospheric current sheet (HCS) drift for any tilt angle based on Parker’s heliospheric magnetic field and compare it with published two-dimensional and quasi-3D methods. We also present a new approach to determine the magnitude of the 3D HCS drift numerically. Implications of these new methods for the solar modulation of Galactic cosmic rays are considered and compared with results from prior methods reported in the literature. Our results support the concept that HCS drift plays an important role in the solar modulation of cosmic rays.

*Key words:* cosmic rays – diffusion – methods: numerical – methods: statistical

*Online-only material:* color figures

### 1. INTRODUCTION

Solar modulation is the process by which the Sun impedes the entry of Galactic cosmic rays (GCRs) into the solar system, thereby altering the intensity and energy spectrum of the cosmic rays. This process is governed by Parker’s equation which includes four different modulation mechanisms: diffusion, convection, adiabatic cooling, and drifts. Convection and adiabatic cooling have been successfully modeled. Determining the diffusion effect is a challenging astrophysical problem, because it requires an understanding of the properties of magnetic fields and turbulence throughout the heliosphere, while also demands accurate theories for determining particle transport properties—such as the diffusion tensor—from the properties of the turbulence (Pei et al. 2010a). Another challenge is to incorporate the drift effects in numerical simulations which is especially difficult in the vicinity of the heliospheric current sheet (HCS).

It is important to consider particle drifts—gradient and curvature drifts as well as drift along the HCS—in modeling cosmic ray transport inside the heliosphere because there is a well-known difference in cosmic ray modulation in successive polarity periods (Jokipii & Levy 1977; Isenberg & Jokipii 1979). Although gradient and curvature drifts are well understood and can be calculated based on the mean magnetic field (see, e.g., Jokipii et al. 1977), a generally accepted model for HCS drift is still elusive. Early approaches (Jokipii et al. 1977; Isenberg & Jokipii 1979; Jokipii & Thomas 1981) take the HCS drift as a  $\delta$ -function limit of the regular gradient and curvature drifts, and implement it as a jump condition. Other approaches include simply neglecting drifts (see, e.g., Jokipii & Levy 1977; Gervasi et al. 1999; Alanko et al. 2003), emulating drift in two-dimensional (2D) models (see, e.g., Potgieter & Moraal 1985), using conservation of drift flux in 2D models (Caballero-Lopez & Moraal 2003), or calculating a 2D drift velocity field (Alanko-Huotari et al. 2007). The exact technique used for HCS drift is not always specified (see, e.g., Kóta & Jokipii 1983; Miyake & Yanagita 2005). See Burger and Potgieter (1989) for a review of a number of models for HCS drift. In the present approach we assume that the three-dimensional (3D) HCS is locally flat and then use the drift velocity field of Burger et al. (1985), derived through particle tracing. The HCS is described by a transcendental function

(Jokipii & Thomas 1981; Kóta & Jokipii 1983; Thomas et al. 1986) which usually makes the simulation prohibitive in terms of computing time if the drift velocity field of Burger et al. (1985) is used in three dimensions. By making suitable assumptions the computing time can however be reduced considerably without compromising accuracy unduly. We investigate the effects of this new approach by comparing solutions of Parker’s equation with a wavy HCS using our newly developed stochastic method (Pei et al. 2010b) against those in the literature (Kóta & Jokipii 1983). Our new approach and the HCS model are presented in Section 2. The stochastic method is briefly discussed in Section 3 for completeness and its results are discussed in Section 4. Finally, Section 5 concludes this article. The evolution of the HCS model is included in the Appendix.

### 2. TRANSPORT MODEL

The governing equation for solar modulation is Parker’s well-known transport equation (Parker 1965; Jokipii & Parker 1970),

$$\frac{\partial f}{\partial t} = \nabla \cdot (\kappa \cdot \nabla f - \mathbf{V}f) + \frac{1}{3p^2} (\nabla \cdot \mathbf{V}) \frac{\partial (p^3 f)}{\partial p}, \quad (1)$$

where  $f(\mathbf{r}, p, t)$  is the omni-directional distribution function (i.e., the phase space density averaged over solid angle in momentum space), with  $p$  the particle momentum,  $\mathbf{r}$  the spatial variable, and  $\mathbf{V}$  the solar wind velocity. Note that we drop the subscript 0 typically used for the omni-directional distribution function. Terms relating to the second-order Fermi acceleration and sources will not be discussed in this paper. The spatial diffusion tensor,  $\kappa$ , can be decomposed into two parts,  $\kappa_s$ , the symmetric part, and  $\kappa_A$ , the anti-symmetric part. The divergence of the anti-symmetric tensor,  $\kappa_A$ , is the drift velocity,  $\mathbf{V}_d$ . The symmetric tensor,  $\kappa_s$ , consists of the spatial diffusion parallel  $\kappa_{\parallel}$  and perpendicular  $\kappa_{\perp}$  to the mean heliospheric magnetic field,  $\mathbf{B}$ , which is given by

$$\mathbf{B} = \frac{A}{r^2} \left( \hat{\mathbf{e}}_r - \frac{(r - r_s)\Omega_{\odot}}{V} \sin\theta \hat{\mathbf{e}}_{\phi} \right) [1 - 2\mathbf{H}(\theta - \theta_{cs})], \quad (2)$$

where  $A = \pm B_0 r_0^2$  is a constant which comes from the definition of the magnetic field, with suffix 0 indicating some reference value and the sign depending on solar cycle, and  $\Omega_{\odot}$

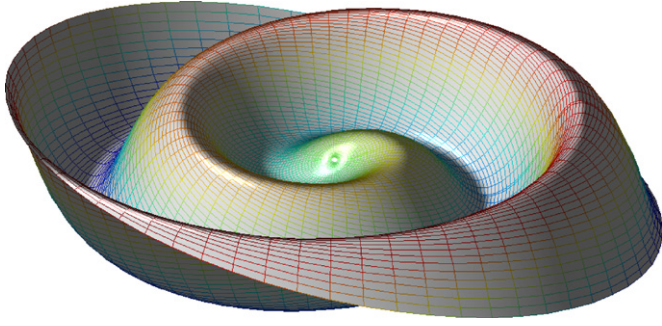


**Figure 1.** Wavy HCS based on Equation (4) displayed out to a radius of 10 AU. (A color version of this figure is available in the online journal.)

is the sidereal solar rotation rate corresponding to a period of 25.4 days. The Heaviside step function is represented by  $H$ . The polar angle of the current sheet,  $\theta_{cs}$ , is determined by Equation (4).

The tilt angle,  $\alpha$ , of the HCS at any radial distance  $r$  is defined to be the maximal latitudinal excursion of the current sheet within a shell of radius  $r$ . We assume that the excursion is the same in the northern and southern hemispheres. Because we allow the tilt angle on the solar source surface to vary with time, the tilt angle at radius  $r$  is related to the tilt angle at the source surface  $r_s$  at some earlier time,

$$\begin{aligned} \alpha(t, r) &= \alpha\left(t - \frac{r - r_s}{V}, r_s\right) \\ &= \alpha_0 \pm \frac{\pi}{11 \text{ years}} \left(t - t_0 - \frac{r - r_s}{V}\right). \end{aligned} \quad (3)$$

The expression after the first equal sign is more general and might be used, for instance, if the time variation of the current sheet is based on observations (Hoeksema et al. 1983). For concreteness, we adopt the expression after the second equal sign, which assumes a linear variation during an 11 year long solar cycle. Here,  $\alpha_0$  is the tilt angle at the source surface at some reference time  $t_0$ . The plus and minus signs apply when the tilt angle is, respectively, increasing or decreasing, and this sign needs to be reversed at the appropriate time in the solar cycle. Note that this version is a modification of Thomas et al. (1986) (see also the Appendix). The full shape of the current sheet in three dimensions is then defined as the surface that satisfies the equation,

$$\begin{aligned} \tan\left(\frac{\pi}{2} - \theta_{cs}\right) &= \tan \alpha(t, r) \sin \left[\phi + \frac{\Omega_{\odot}(r - r_s)}{V} - \Omega_{\odot}(t - t_0)\right] \\ &= \tan \alpha(t, r) \sin \phi_0 \end{aligned} \quad (4)$$

where  $\phi_0 = \phi + (r - r_s)\Omega_{\odot}/V - \Omega_{\odot}(t - t_0)$ . Note that Equation (4) is valid for any tilt angle but that we use modest tilt angles appropriate for conditions near solar minimum. Jokipii & Thomas (1981) presented an approximation to this equation which uses sine instead of tangent for a small tilt angle, i.e.,  $\alpha(t, r) < 5^\circ$ . However, even today many publications use this approximation for much larger  $\alpha(t, r)$  than its domain of validity, rather than the correct formula displayed in Equation (4) (Kóta & Jokipii 1983; Thomas et al. 1986). Generally speaking, the shape of the HCS is changing with time and position. In this paper, we “freeze” the HCS at time  $t_0$  and take a snapshot of it (see Figure 1) in order to compare our results with Kóta & Jokipii (1983).

The parallel diffusion component,  $\kappa_{\parallel}$ , and the perpendicular component,  $\kappa_{\perp}$ , can be determined ab initio from turbulence models based on spacecraft measurements (Pei et al. 2010a).

The general weak-scattering drift velocity of a particle with charge  $q$ , momentum  $p$ , and speed  $v$  is given by Jokipii et al. (1977),

$$\begin{aligned} \mathbf{V}_d &= \frac{pv}{3q} \nabla \times \left(\frac{\mathbf{B}}{B^2}\right) = \frac{2pv(r - r_s)}{3qA(1 + \gamma^2)^2} [1 - 2H(\theta - \theta_{cs})] \\ &\quad \times \left[-\frac{\gamma}{\tan \theta} \hat{\mathbf{e}}_r + (2 + \gamma^2)\gamma \hat{\mathbf{e}}_{\theta} + \frac{\gamma^2}{\tan \theta} \hat{\mathbf{e}}_{\phi}\right], \end{aligned} \quad (5)$$

where  $\gamma = (r - r_s)\Omega_{\odot} \sin \theta / V$ . This formula is valid for particles away from the HCS and is the summation of the curvature drift and the gradient drift. For the drift near the HCS, an additional term is added,

$$\mathbf{V}_{dc} = \frac{2pv(r - r_s)}{3qA(1 + \gamma^2)} \delta(\theta - \theta_{cs})(\gamma \hat{\mathbf{e}}_r + \hat{\mathbf{e}}_{\phi}).$$

However, we replace the  $\delta$ -function approximation with an improved formula shown below in Equation (6).

### 2.1. HCS Drift

For the current sheet drift speed/magnitude, we adopt a formula following Burger (1987),

$$V_{dc} = \left[0.457 - 0.412 \left(\frac{d}{R_g}\right) + 0.0915 \left(\frac{d}{R_g}\right)^2\right] v, \quad (6)$$

where  $d$  is the distance to the current sheet and  $R_g$  is the Larmor radius. This formula follows from a fit by Burger (1987) to Figure 4 of Burger et al. (1985), who used particle trajectory tracing to calculate the drift velocity field for an isotropic distribution of particles drifting along a flat current sheet. Note that this formula is valid when  $d$  is smaller than two times  $R_g$ . We assume that the wavy HCS is locally flat. We should emphasize that the Parker transport equation does not contain information about the motion of individual particles. Moreover, in the presence of scattering, the trajectories of the particles that contribute to the distribution at any given position will certainly be displaced randomly from the unperturbed trajectories. Therefore individual particles will typically not succeed in drifting along the wavy current sheet for long distances (see Strauss et al. 2011). One would also expect that they will short circuit the regions of the current sheet where their Larmor radii are larger than the spatial scale over which the wavy neutral sheet changes, typically near the crests and troughs of the sheet, where the assumption of local flatness is clearly not valid. Away from these regions of maximum extent of the wavy current sheet the assumption of local flatness is more realistic. In any case, the fraction of the wavy current sheet where the assumption of local flatness fails is smaller than the fraction of the sheet where it is a reasonable assumption and becomes even smaller as the tilt angle increases.

By definition the HCS drift is perpendicular to the magnetic field and is parallel to the local current sheet. At each point  $(r, \theta_{cs}, \phi)$  on the field line which resides in the current sheet, the tangent is  $(dr, r d\theta, r \sin \theta_{cs} d\phi)$  which is  $(V, 0, -r \sin \theta_{cs} \Omega_{\odot})$  for the Parker field. Locally the normal vector of the HCS,  $\mathbf{n}$ , is given by

$$n_r = -\frac{\Omega_{\odot}}{V} \tan \alpha(t, r) \cos \phi_0 \pm \frac{\sec^2 \alpha(t, r)}{V} \frac{\pi}{11 \text{ years}} \sin \phi_0, \quad (7)$$

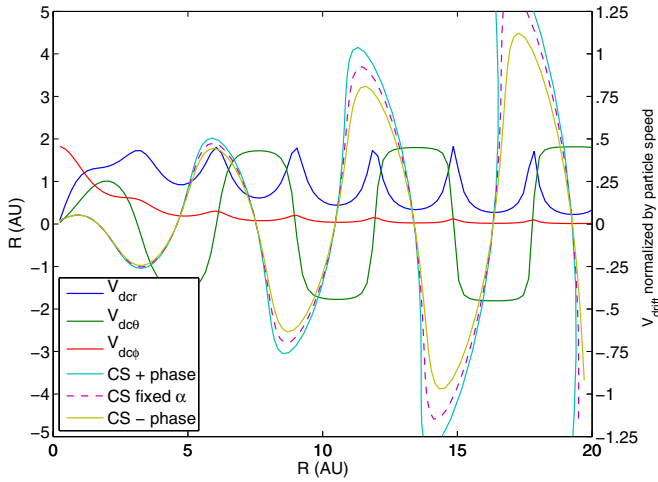


**Figure 2.** Wavy HCS drift for a fixed  $\phi$ . “CS” denotes the current sheet. “+ phase” means we take the positive sign in Equation (3) after  $\alpha_0$ . “- phase” means we take the negative sign in that equation. The drift velocity components plotted in this figure and others are all normalized by the particle speed. The wavy current sheet is plotted with respect to the left and bottom axes and the components of the normalized drift velocity are plotted with respect to the right and bottom axes.

(A color version of this figure is available in the online journal.)

$$n_\theta = -\frac{\csc^2 \theta_{cs}}{r}, \quad (8)$$

$$n_\phi = -\frac{\tan \alpha(t, r) \cos \phi_0}{r \sin \theta_{cs}}. \quad (9)$$

Note that if we use a fixed tilt angle throughout the heliosphere as in Kóta & Jokipii (1983), we have the normal vector as

$$n_r = -\frac{\Omega_\odot}{V} \tan \alpha_0 \cos \phi_0 \quad (10)$$

$$n_\theta = -\frac{\csc^2 \theta_{cs}}{r}, \quad (11)$$

$$n_\phi = -\frac{\tan \alpha_0 \cos \phi_0}{r \sin \theta_{cs}}. \quad (12)$$

By considering Equations (2)–(4) and (7)–(9), we find that the three components of the current sheet drift velocity for a 3D wavy HCS are given by

$$\begin{aligned} V_{dcr} &= \frac{r \sin \theta_{cs} \Omega_\odot V_{dc}}{\sqrt{V^2 + V_{\theta x}^2 + r^2 \sin^2 \theta_{cs} \Omega_\odot^2}}, \\ V_{dc\theta} &= -\frac{\tan \alpha(t, r) \sin \theta_{cs} \cos \phi_0 (V^2 + r^2 \sin^2 \theta_{cs} \Omega_\odot^2) V_{dc}}{\sqrt{V^2 + V_{\theta x}^2 + r^2 \sin^2 \theta_{cs} \Omega_\odot^2} V}, \\ V_{dc\phi} &= \frac{V V_{dc}}{\sqrt{V^2 + V_{\theta x}^2 + r^2 \sin^2 \theta_{cs} \Omega_\odot^2}}, \end{aligned} \quad (13)$$

where  $V_{\theta x}$  is given by

$$\begin{aligned} V_{\theta x} &= -\frac{\tan \alpha(t, r) \sin \theta_{cs} \cos \phi_0}{V} (V^2 + r^2 \sin^2 \theta_{cs} \Omega_\odot^2) \\ &\pm \frac{\pi}{11 \text{ years}} \frac{r^2 \sin^3 \theta_{cs} \Omega_\odot}{V} \sin \phi_0 \sec^2 \alpha(t, r), \end{aligned} \quad (14)$$

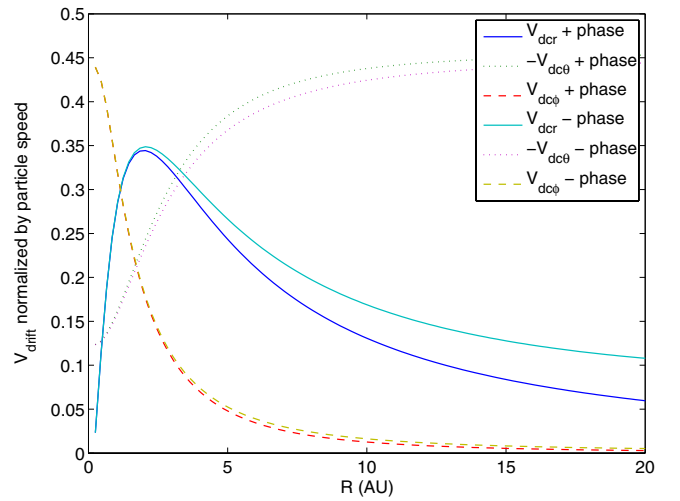


**Figure 3.** Wavy HCS drift along a field line with  $\alpha_0 = 18^\circ$ .

(A color version of this figure is available in the online journal.)

for the Parker magnetic field and for a time-dependent tilt angle. Note that Equation (13) in this article is different from Equation (3) in Caballero-Lopez & Moraal (2003) which projects the components of the HCS drift into two planes. If those two planes are perpendicular to each other then it is a true 3D result which is approximately true for  $r > 20$  AU. Therefore we believe the formula in Caballero-Lopez & Moraal (2003) is quasi-3D.

After we obtain  $d$  for Equation (6), we can determine all the three components according to Equation (13). Note that Equation (13) is derived analytically based on the shape of the HCS without further assumptions and is valid for large tilt angle. That is to say that if we have a better formula than Equation (6), we can still use Equation (13) with a different  $V_{dc}$ . If we choose a different heliospheric magnetic field, we could just change the value of the tangent of the field line and the normal vector of the HCS and find the corresponding directions of the HCS drift components.

The distance  $d$  is given by

$$d = \min \left[ \sqrt{(x_1 - x_0)^2 + (y_1 - y_0)^2 + (z_1 - z_0)^2} \right], \quad (15)$$

where  $(x_0, y_0, z_0)$  denotes the coordinates of any point on the current sheet and  $(x_1, y_1, z_1)$  denotes an arbitrary position in the heliosphere. To determine the distance  $d$  according to Equation (15), we discretize the wavy HCS into a 2D mesh (586 nodes in the radial direction for an approximately  $2\pi$  period and 180 nodes in the polar direction in this paper) for the HCS in a 2D surface as shown in Figure 1.

We can reduce the calculation time basing on the fact that  $r$  is periodic on the current sheet surface which can be shown by Equation (4) if time is fixed and by Figures 2 and 3. Therefore in radial direction, we only need 586 points to achieve a resolution of  $\delta r = 0.01$  AU. Then we can calculate the distance between all the points (586 times 180) to  $(x_1, y_1, z_1)$  on the mesh and find the minimum which is  $d$ .

Since the line of the shortest distance must be normal to the wavy HCS, it is not necessary to calculate the distance from  $(x_1, y_1, z_1)$  to all the points on the mesh. For example, if  $r > 20$  AU, the radial direction is almost normal to the HCS near the equatorial plane. Therefore in this case, the difference between the azimuthal angle of  $(x_0, y_0, z_0)$  and  $(x_1, y_1, z_1)$  is very small.

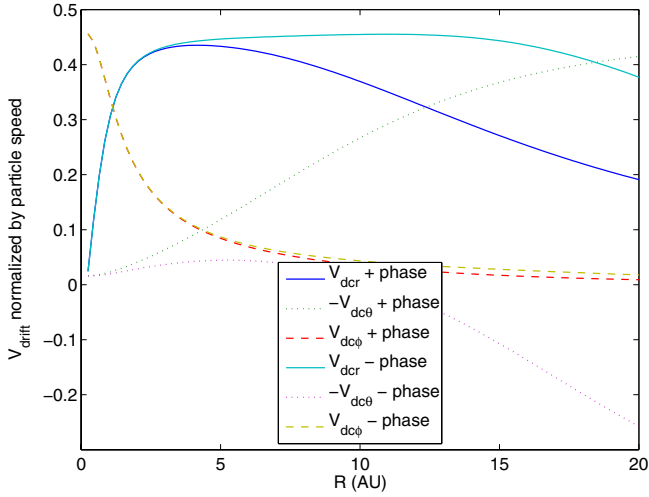


**Figure 4.** Wavy HCS drift along a field line with  $\alpha_0 = 2^\circ$ .  
(A color version of this figure is available in the online journal.)

### 3. NUMERICAL MODEL

The stochastic method to solve Equation (1) can be divided into two steps. The first step is that we need to find the corresponding stochastic differential equations (SDEs) to Equation (1) based on Ito's formula (Ito 1951) and solve it. The second step is that we obtain the modulated distribution function from the solutions of the corresponding SDEs (Pei et al. 2010b).

The equivalent SDEs to Equation (1) are

$$\Delta r = \left( \frac{1}{r^2} \frac{\partial r^2 \kappa_{rr}}{\partial r} + \frac{1}{r \sin \theta} \frac{\partial \kappa_{r\phi}}{\partial \phi} + V + V_{dr} \right) \Delta t + [\mathbf{B} \cdot \Delta \mathbf{W}]_r, \quad (16)$$

$$\Delta \theta = \frac{1}{r^2 \sin \theta} \frac{\partial \sin \theta \kappa_{\theta\theta}}{\partial \theta} \Delta t + \frac{V_{d\theta}}{r} \Delta t + [\mathbf{B} \cdot \Delta \mathbf{W}]_\theta, \quad (17)$$

$$\Delta \phi = \frac{1}{r^2 \sin^2 \theta} \frac{\partial \kappa_{\phi\phi}}{\partial \phi} + \frac{1}{r^2 \sin \theta} \frac{\partial r \kappa_{r\phi}}{\partial r} \Delta t + \frac{V_{d\phi}}{r \sin \theta} \Delta t + [\mathbf{B} \cdot \Delta \mathbf{W}]_\phi, \quad (18)$$

$$\Delta p = -\frac{p}{3r^2} \frac{\partial r^2 V}{\partial r} \Delta t. \quad (19)$$

The calculation of  $\mathbf{B} \cdot \Delta \mathbf{W}$  can be done similarly as in Pei et al. (2010b).

We choose backward-in-time method to integrate the SDEs (Equations (16)–(19)). All modulation parameters and boundary conditions are taken to be the same as given in Kóta & Jokipii (1983). More details of how to solve Equation (1) and how to determine the modulated spectrum of cosmic rays by using the stochastic method can be found in Pei et al. (2010b).

### 4. RESULTS

The components of the HCS drift are shown in Figures 2–4. These figures apply to a particle right on the current sheet, i.e.,  $d = 0$  in Equation (6). Figure 2 shows the components of the HCS drift when  $\phi$  is a constant and the tilt angle is  $18^\circ$ . The dashed

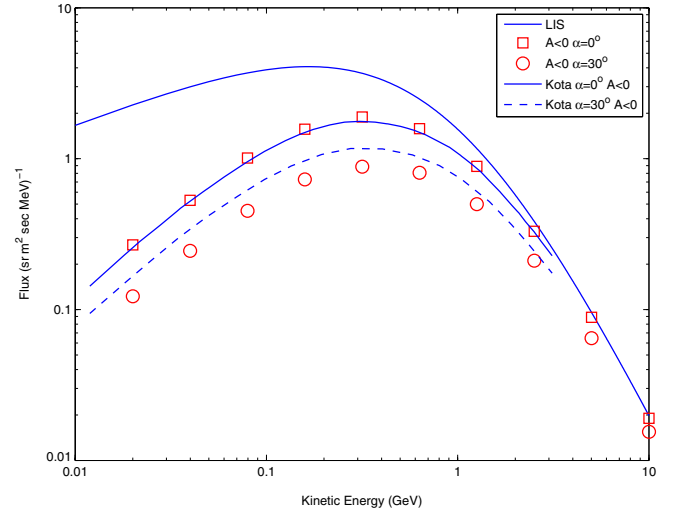


**Figure 5.** Comparisons between our results with those in Kóta & Jokipii (1983).  
(A color version of this figure is available in the online journal.)

line is the HCS with a fixed, i.e., time-independent, tilt angle. In this figure, we can see that the time-dependent tilt angle clearly affects the shape of the current sheet. For example, at about 12 AU, the peak of the increasing phase is about 1 AU larger than that of the decreasing phase. The difference becomes even larger with the increasing radial distance. However, the time-dependent tilt angle has a much smaller effect on the magnitude of the drift speeds. Therefore we only plot the drift speeds for the increasing phase.

Figures 3 and 4 show the components of the HCS drift when  $\theta$  is a constant, and where  $\phi$  and  $r$  are varying in the same way as a Parker field line. One is for a tilt angle of  $18^\circ$ , the other for  $2^\circ$ . Note that in these two figures,  $V_{d\theta}$  is negated. The time-dependent tilt angle shows a more evident effect on  $V_{dcr}$  than two other components in Figure 3. But the time-dependent tilt angle shows a very weak effect on  $V_{dc\phi}$  on both Figures 3 and 4. Figure 4 shows a dramatic effect of the time-dependent feature of the tilt angle where  $V_{dc\theta}$  even change sign at about 11 AU for different phases.

The features shown in Figures 2–4 are different from those shown in Figure 4 in Alanko-Huotari et al. (2007). First of all, the normalized  $V_{dcr}$  is independent of energy. Second, the components of the drift velocity oscillate along the wavy current sheet if we keep  $\phi$  a constant as shown in Figure 2. Third, the normalized  $V_{dcr}$  is a smooth function of  $r$  whose maximum is reached at about 1.8 AU and then decreases all the way to 100 AU during the positive phase as shown in Figures 3 and 4 if we follow the field line close to the wavy current sheet, i.e., with a fixed  $\theta$ . For the negative phase,  $V_{dcr}$  is similar if the tilt angle is not small (see Figure 3). However,  $V_{dcr}$  is totally different during the negative phase as shown in Figure 4.

To see the 3D HCS drift effect on the modulation of GCRs, we compare our results with those in Kóta & Jokipii (1983) which has a wavy HCS but with a different HCS drift. All other parameters are the same. The modulated spectra observed at 1 AU are shown in Figure 5. The lines are taken from Kóta & Jokipii (1983). From this figure, we can see that our results agree very well with Kóta & Jokipii (1983) for the tilt angle of  $0 \text{ deg}^2$ . The modulated spectra for  $\alpha = 30^\circ$  according to our method (circles) are lower than those in Kóta & Jokipii (1983). However, our results are supported by a totally different new analytical method presented in Burger (2011) which shows

that the difference between the spectra obtained by the two approaches are less than 5%. The reason for this difference may come from two facts. (1), In Kóta & Jokipii (1983), they determine the HCS drift totally numerically. We determine the directions analytically; (2), In Kóta & Jokipii (1983), the magnitude of the HCS drift is also determined numerically. We use the formula given by Burger et al. (1985) and Burger (1987). We note that while in the current paper we assume that the wavy current sheet is locally flat, this assumption is not made in Burger (2011). The good agreement suggests that the assumption of local flatness does not have as large an affect on our results as one might have expected, at least for the parameter set used in the comparison.

## 5. CONCLUSION

We present the method on how to analytically determine the directions of the 3D HCS drift based on the Parker field for the first time so far as we know. We also present a new way to determine the magnitude of the HCS drift using an improved method for computing the distance of the closest approach of the current sheet. By combining these two methods, we show that the 3D HCS drift is important for low energy particles and the modulation is stronger by comparing our results to results in the literature which means that it is possible that the 2D HCS drift or the quasi-3D HCS drift underestimate the modulation effect. We argue that the assumption that the wavy current sheet is locally flat is reasonable and does not invalidate our results.

We also note that our methods are extensible to other magnetic field configurations and to other approaches to determine the magnitude of the HCS drift.

This work was supported in part by NASA EPSCoR Cooperative Agreement NNX09AB05A, NASA Heliophysics Theory grant NNX08AI47G, the Charged Sign Dependence grant NNX08BA62G, and by the South African National Research Foundation.

## APPENDIX

### THE EVOLUTION OF THE MODEL FOR THE HCS

First presented in Jokipii & Thomas (1981), the formula for the current sheet is

$$\sin\left(\frac{\pi}{2} - \theta\right) = -\sin\alpha \sin\left(\phi - \phi_0 + \frac{\Omega_{\odot} r}{V}\right), \quad (\text{A1})$$

which is valid for a small tilt angle, i.e.,  $\alpha < 5^{\circ}$ . However, many researchers used this formula and ignored the small tilt angle requirement. Two years later a more rigorously form was published by Kóta & Jokipii (1983) which is appropriate for any tilt angle in the corotating frame,

$$\cot\theta^* = -\tan\alpha \sin\phi^*, \quad (\text{A2})$$

which  $\theta^*$  and  $\phi^*$  are measured in the corotating frame.

In the fixed frame Equation (A2) is

$$\cot\theta = -\tan\alpha \sin\left(\phi + \frac{\Omega_{\odot} r}{V}\right), \quad (\text{A3})$$

which is a special case of Equation (2) in Thomas et al. (1986),

$$\cot\theta = -\tan\alpha(t) \sin\left(\phi - \phi_0 + \frac{\Omega_{\odot} r}{V}\right), \quad (\text{A4})$$

where the time dependence of  $\alpha(t)$  is also assumed to be

$$\alpha(t) = \frac{\pi t}{11 \text{ years}}. \quad (\text{A5})$$

With the source surface radius, the time dependence, and the initial condition being considered, we have Equations (3) and (4) in this paper.

## REFERENCES

- Alanko, K. M., Usoskin, I., Mursula, K., & Kovaltsov, G. A. 2003, in Int. Cosmic Ray Conf. on a 2D Stochastic Simulation of Galactic Cosmic Rays Transport in the Heliosphere, Vol. 7, 3851
- Alanko-Huotari, K., Usoskin, I. G., Mursula, K., & Kovaltsov, G. A. 2007, *J. Geophys. Res. (Space Phys.)*, 112, 8101
- Burger, R. A. 1987, PhD thesis, Potchefstroomse Universiteit vir Christelike Hoër Onderwys, Republic of South Africa
- Burger, R. A. 2011, *ApJ*, submitted
- Burger, R. A., Moraal, H., & Webb, G. M. 1985, *Ap&SS*, 116, 107
- Burger, R. A., & Potgieter, M. S. 1989, *ApJ*, 339, 501
- Caballero-Lopez, R. A., & Moraal, H. 2003, in Int. Cosmic Ray Conf. on the Numerical Description of Neutral Sheet Drift Effects, Vol.7, 3871
- Gervasi, M., Rancoita, P. G., Usoskin, I. G., & Kovaltsov, G. A. 1999, *Nucl. Phys. B*, 78, 26
- Hoeksema, J. T., Wilcox, J. M., & Scherrer, P. H. 1983, *J. Geophys. Res.*, 88, 9910
- Isenberg, P. A., & Jokipii, J. R. 1979, *ApJ*, 234, 746
- Ito, K. 1951, *Mem. Amer. Math. Soc.*, 4, 1
- Jokipii, J. R., & Levy, E. H. 1977, *ApJ*, 213, L85
- Jokipii, J. R., & Parker, E. N. 1970, *ApJ*, 160, 735
- Jokipii, J. R., & Thomas, B. 1981, *ApJ*, 243, 1115
- Jokipii, J. R., Levy, E. H., & Hubbard, W. B. 1977, *ApJ*, 213, 861
- Kóta, J., & Jokipii, J. R. 1983, *ApJ*, 265, 573
- Miyake, S., & Yanagita, S. 2005, in Int. Cosmic Ray Conf. on Effects of the Tilted and Wavy Current Sheet on the Solar Modulation of Galactic Cosmic Rays, Vol.2, 101
- Parker, E. N. 1965, *Planet. Space Sci.*, 13, 9
- Pei, C., Bieber, J. W., Breech, B., et al. 2010a, *J. Geophys. Res. (Space Phys.)*, 115, 3103
- Pei, C., Bieber, J. W., Burger, R. A., & Clem, J. 2010b, *J. Geophys. Res. (Space Phys.)*, 115, 12107
- Potgieter, M. S., & Moraal, H. 1985, *ApJ*, 294, 425
- Strauss, R. D., Potgieter, M. S., Büsching, I., & Kopp, A. 2011, *ApJ*, 735, 83
- Thomas, B. T., Goldstein, B. E., & Smith, E. J. 1986, *J. Geophys. Res.*, 91, 2889